AIP | Journal of Applied Physics

Defects in 30 keV Er + -implanted SiO 2 /Si studied by positron annihilation and cathodoluminescence

K. Hirata, H. Arai, A. Kawasuso, T. Sekiguchi, Y. Kobayashi, and S. Okada

Citation: Journal of Applied Physics **90**, 237 (2001); doi: 10.1063/1.1371948
View online: http://dx.doi.org/10.1063/1.1371948
View Table of Contents: http://scitation.aip.org/content/aip/journal/jap/90/1?ver=pdfcov
Published by the AIP Publishing

Articles you may be interested in

Positron beam studies of argon-irradiated polycrystal α - Zr
J. Appl. Phys. **97**, 063511 (2005); 10.1063/1.1833573

Vacancies and deep levels in electron-irradiated 6H SiC epilayers studied by positron annihilation and deep level transient spectroscopy
J. Appl. Phys. **90**, 3377 (2001); 10.1063/1.1402144

Buried oxide and defects in oxygen implanted Si monitored by positron annihilation
J. Appl. Phys. **90**, 1179 (2001); 10.1063/1.1380411

Low temperature annealing of 4H–SiC Schottky diode edge terminations formed by 30 keV Ar + implantation
J. Appl. Phys. **87**, 3973 (2000); 10.1063/1.372443

He-implantation induced defects in Si studied by slow positron annihilation spectroscopy
J. Appl. Phys. **85**, 2390 (1999); 10.1063/1.369555

[This article is copyrighted as indicated in the article. Reuse of AIP content is subject to the terms at: http://scitation.aip.org/termsconditions. Downloaded to] IP: 157.111.48.196 On: Sat, 30 Jan 2016 06:38:52

Defects in 30 keV Er^+-implanted SiO_2/Si studied by positron annihilation and cathodoluminescence

K. Hirata[a)]
National Institute of Advanced Industrial Science and Technology (AIST), 1-1-1 Higashi, Tsukuba, Ibaraki 305-8565, Japan

H. Arai[b)] and A. Kawasuso
Japan Atomic Energy Research Institute, 1233 Watanuki, Takasaki, Gunma 370-12, Japan

T. Sekiguchi[c)]
Institute for Materials Research, Tohoku University, Sendai 980-77, Japan

Y. Kobayashi
National Institute of Advanced Industrial Science and Technology (AIST), 1-1-1 Higashi, Tsukuba, Ibaraki 305-8565, Japan

S. Okada
Japan Atomic Energy Research Institute, 1233 Watanuki, Takasaki, Gunma 370-12, Japan

(Received 25 July 2000; accepted for publication 21 March 2001)

Defects in SiO_2 (48 nm)/Si induced by 30 keV Er ion implantation were studied by positron annihilation. Depth-selective information on defects for samples implanted with doses of 3.0×10^{14} and 1.5×10^{15} Er/cm^2 was obtained by a variable-energy positron beam by measuring Doppler broadening of positron annihilation γ rays as a function of incident positron energy. Comparison of the results by Doppler broadening with those by electron spin resonance after annealing indicates that the types of defects (which predominantly exist in the SiO_2 layer) depend on implantation dose. The annealing temperature dependence of positron data is compared with that of the cathodoluminescence intensity at 1.54 μm, and the possible effect of defects on luminescence intensity is discussed. © *2001 American Institute of Physics.* [DOI: 10.1063/1.1371948]

I. INTRODUCTION

Er-doped SiO_2 fiber has been used as the main component of optical amplifiers,[1] because the trivalent cation of Er exhibits luminescence at a wavelength of 1.54 μm,[2,3] which corresponds to the maximum transparency of silica-based optical fibers. An electroluminescence device was also fabricated using Er-doped SiO_2 in a silicon-based metal-oxide semiconductor.[4] As the SiO_2 layer was 50 nm or less thick, Er ions were implanted into it at an energy of 50 keV, so that all implanted ions stopped in the SiO_2 layer. However, defects introduced during the slowing down process of implanted ions have an influence on the luminescence intensity and proper control of defects is very important to develop high performance luminescence devices.[5–7]

In the present work, we applied the positron annihilation technique to study defects generated by 30 keV Er ions implanted into a thin SiO_2 layer (48 nm) grown on a Si substrate. Positron annihilation is very useful to study defects and damage because of its high sensitivity.[8–13] Cathodoluminescence (CL) was also measured as a function of annealing temperature and the possible effect of defects on luminescence intensity in a SiO_2/Si system suitable for an electroluminescence device is discussed.

II. EXPERIMENTS

Silicon dioxide (SiO_2) films with a thickness of 48 nm were grown on floating-zone Si (100) substrates by dry oxidation at 1100 °C. Samples were implanted with 30 keV Er ions at doses of 3.0×10^{14} and 1.5×10^{15} Er/cm^2 using a 400 keV ion implantation system of the Japan Atomic Energy Research Institute (JAERI)/Takasaki.[14] The implantation energy was chosen based on transport of ions in matter (TRIM)[15] calculations to stop all ions at the SiO_2 layer (TRIM calculations gave an average Er implantation depth of 21 nm). Successive postimplantation annealing was conducted between 300 and 900 °C for 30 min in an argon atmosphere.

The energy distribution of positron annihilation γ rays was measured using a magnetically guided variable-energy positron beam.[16] The positron energy was varied from 80 eV to 30 keV. The Doppler spectrum recorded with a high resolution Ge detector (EG&G Ortec GEM 18180P) was characterized by the S parameter, which was the ratio of γ-ray counts in the central part of the 511 keV annihilation peak to the total counts contained in the whole peak. We defined the S parameter as the ratio of counts between 510.3 and 511.7 keV to those between 506.8 and 515.2 keV.

[a)]Author to whom correspondence should be addressed; electronic mail: k.hirata@aist.go.jp
[b)]Ishikawajima-Harima Heavy Industries Co., Ltd., Yokohama 235-8501, Japan.
[c)]National Institute for Materials Science, Tsukuba 305-0047, Japan.

 © 2001 American Institute of Physics
[This article is copyrighted as indicated in the article. Reuse of AIP content is subject to the terms at: http://scitation.aip.org/termsconditions. Downloaded to] IP: 157.111.48.196 On: Sat, 30 Jan 2016 06:38:52

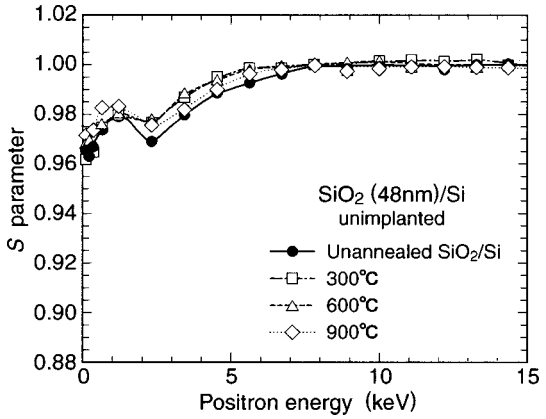

FIG. 1. Annealing temperature dependence of *S-E* curves for unimplanted SiO_2 (48 nm)/Si. The *S-E* curves of the unimplanted SiO_2/Si are not changed by annealing.

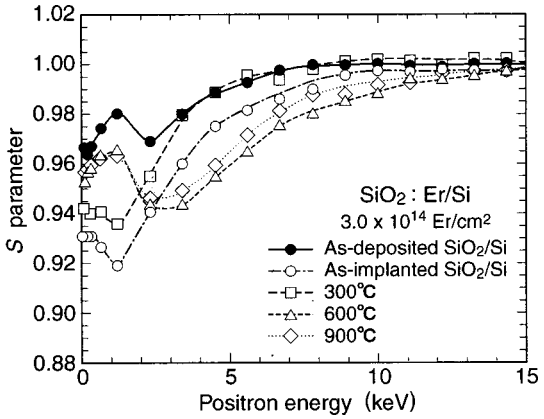

FIG. 2. Annealing temperature dependence of *S-E* curves for Er-implanted SiO_2/Si (dose: $\Phi = 3.0\times10^{14}$ Er/cm^2).

To characterize optical properties of Er-implanted SiO_2/Si, cathodoluminescence (CL) was measured at room temperature. A scanning electron microscope (TOPCON DS-130) was modified for CL measurement. Luminescence emitted by accelerated electrons was collected by an ellipsoidal mirror and led to a monochrometer (Jobin Yvon HR 320) via an optical fiber. Luminescence was detected by a Ge *p-i-n* diode (North Coast EO-817L). Signals were accumulated and analyzed with a personal computer as described elsewhere.[17] The accelerating voltage was 10 kV and the electron beam current 10–15 nA.

III. RESULTS AND DISCUSSION

A. Defects in the SiO_2 layer

S parameters as a function of positron energy *E* (*S-E* curve) for unimplanted SiO_2/Si at different annealing temperatures are shown in Fig. 1. *S* parameters are normalized to the value for bulk Si at $E > 20$ keV. With decreasing positron energy from 15 keV, the *S* parameter gradually decreases from the bulk value of 1, shows a dip at 2.3 keV, peaks at 1.2 keV, and approaches 0.96 at $E = 80$ eV. The shape of the *S-E* curves in Fig. 1 is typical for SiO_2/Si.[13] The dip at 2.3 keV is due to positron annihilation in the SiO_2/Si interface. As positron energy approaches 2.3 keV, *S* gradually decreases due to positron diffusion back to the interface. The enhancement in *S* around 1.2 keV is attributed to positronium (Ps) formation in the SiO_2 layer.[18]

Ps is the bound state between a positron and an electron. Because of the two possible spin orientations of the two particles, there are two substates of Ps: singlet *para*-positronium (*p*-Ps) and triplet *ortho*-positronium (*o*-Ps).[19] Spin statistics makes the ratio of *p*-Ps and *o*-Ps formation 1:3 in most cases. Although spin-antiparallel *p*-Ps undergoes self-annihilation with a short lifetime of 125 ps, spin-parallel *o*-Ps undergoes pickoff annihilation, in which the positron annihilates with one of the surrounding electrons with an opposite spin. Hence, the γ rays emitted upon *o*-Ps annihilation, similar to those emitted upon free positron annihilation, broaden due to the large momentum associated with annihilating electrons. In contrast, annihilation of thermalized *p*-Ps yields a low momentum and gives a narrow γ-ray energy distribution. The Doppler broadening spectrum is thus strongly influenced by Ps formation; the more Ps formed, the narrower the distribution. This means that the *S* parameter increases with increasing Ps formation.

Figures 2 and 3 show the annealing temperature dependence of *S-E* curves for Er-implanted SiO_2/Si at doses of 3.0×10^{14} and 1.5×10^{15} Er/cm^2. *S* parameters at 1.2 keV for as-implanted samples are reduced in comparison with corresponding values for the unimplanted sample, indicative of suppressed Ps formation in the SiO_2 layer.[20] According to the spur reaction model, Ps forms as a result of recombination between a positron and one of the electrons, released from the surrounding atoms by the positron itself in the terminal spur. Positron-electron recombination must compete with other processes and Ps formation is influenced by various processes in the spur.[21] The presence of dips at 1.2 keV shows that defects introduced due to Er implantation in the SiO_2 layer interfere with Ps formation. We consider that these defects trap a spur positron or electron, which would otherwise form Ps by recombination.

S parameters in the SiO_2 layer measured at $E = 1.2$ keV are plotted versus annealing temperature in Fig. 4. The *S* parameter for the as-implanted 3.0×10^{14} Er/cm^2 sample is

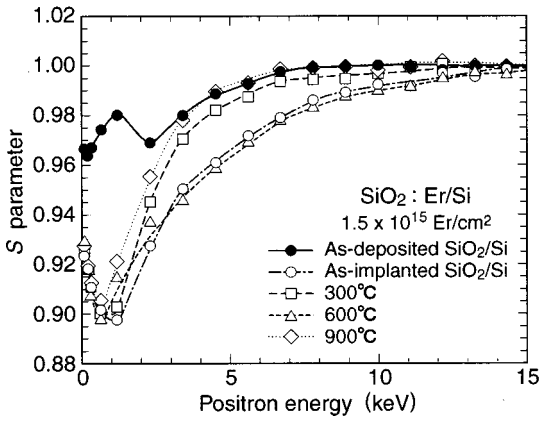

FIG. 3. Annealing temperature dependence of *S-E* curves for Er-implanted SiO_2/Si (dose: $\Phi = 1.5\times10^{15}$ Er/cm^2).

[This article is copyrighted as indicated in the article. Reuse of AIP content is subject to the terms at: http://scitation.aip.org/termsconditions. Downloaded to] IP: 157.111.48.196 On: Sat, 30 Jan 2016 06:38:52

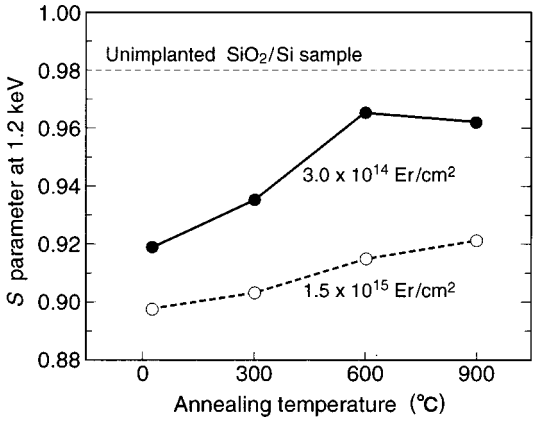

FIG. 4. Variations of normalized S parameters at 1.2 keV for the SiO_2 layer of Er-implanted samples with doses of 3.0×10^{14} and 1.5×10^{15} Er/cm^2 as a function of annealing temperature.

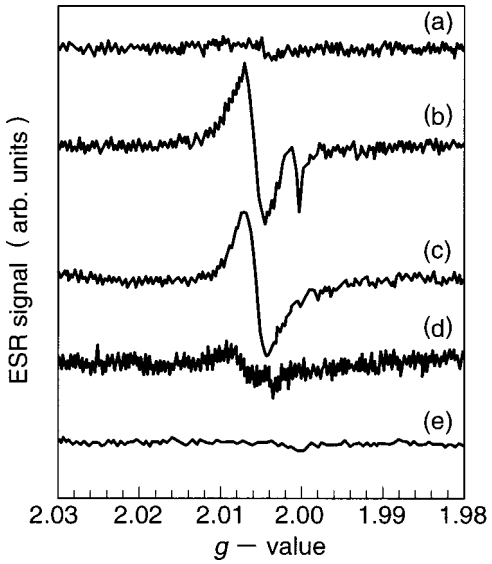

FIG. 5. ESR spectrum measured at room temperature for as-grown SiO_2/Si [spectrum (a)] and Er-implanted ($\Phi=1.5\times10^{15}$ Er/cm^2) SiO_2/Si [spectrum (b)]. ESR spectra for (c) SiO_2 layer removed and the annealed [(d) 600 °C, (e) 900 °C] Er-implanted ($\Phi=1.5\times10^{15}$ Er/cm^2) SiO_2/Si are also shown for comparison.

0.92. Annealing of the sample at 600 °C increases this to 0.97, indicative of the significant recovery of defects at this temperature. Hasegawa *et al.* extensively studied neutron and electron irradiated silica glass by positron annihilation and electron spin resonance (ESR).[22] Most of ESR-detectable damage, E' centers, peroxy radicals, and non-bridging oxygen hole centers, are annihilated upon annealing at 600 °C. They also found that Ps formation in irradiated samples increased progressively after a series of annealing at increased temperatures and returned to the level for the unirradiated sample at 600 °C. The annealing temperature dependence in Fig. 4 thus agrees with their data. We conclude that defects introduced by the 3.0×10^{14} Er/cm^2 implantation into the SiO_2 layer are dominantly ESR detectable, as in the case of neutron and electron irradiated silica.

Note in Fig. 4 that the recovery of the S parameter for the 1.5×10^{15} Er/cm^2 sample is much smaller than that for the 3.0×10^{14} Er/cm^2 sample. The S parameter for the former sample is only 0.93 after annealing at 900 °C. Additional information on the recovery of defects for this sample was obtained by ESR at room temperature with an X-band (9 GHz) microwave incident on a TE_{110} cylindrical cavity using a JEOL JES-TE300 spectrometer. Figure 5 shows an ESR spectrum for the as-implanted 1.5×10^{15} Er/cm^2 sample along with spectra for unimplanted, annealed, and SiO_2-layer-removed samples. In spectrum (b) for the as-implanted sample, two peaks are observed at g of 2.0006 and 2.0055. The peak at $g=2.0006$ is assigned to the E' center in the SiO_2 layer, and that at 2.0055, which remains after removing the SiO_2 layer [spectrum (c)], is attributed to dangling bonds in the amorphized Si substrate based on the g of 2.0055. As is seen in spectrum (d), the peak for E' center disappears after annealing at 600 °C.

The above results indicate that ESR-undetectable defects, responsible for suppressing Ps formation but not annealed out at 900 °C, are dominantly introduced into the SiO_2 layer by 1.5×10^{15} Er/cm^2 implantation. We may consider two defect candidates: (a) hardly recoverable structural modification produced by heavy-ion implantation at a high dose, and (b) Er ions in the SiO_2 network. At a fixed implantation energy, nuclear energy loss of implanted ions, related to collisional events, increases with increasing implanted ion mass. At a high dose of 1.5×10^{15} Er/cm^2, which is so high that the Si substrate is amorphized (see below), the structure of the SiO_2 layer is likely to be destroyed. The atomic-collision-induced structural defects require an annealing temperature close to the original growth temperature to recover the initial structural properties,[23] suggesting that an annealing temperature as high as 1100 °C is required to increase the S parameter in the SiO_2 matrix. On the other hand, implanted Er atoms mainly exist as trivalent positive ions in the SiO_2 network after annealing at 900 °C.[7] Er ions may influence Ps formation probability by trapping Ps precursors or the disappearance of spaces in which Ps is formed. As mentioned above, the spur reaction model states that Ps is formed due to recombination of a thermalized positron-electron pair in the terminal spur. Certain positively charged ions are known to trap Ps precursors[24,25] and it is conceivable that Er ions are responsible for suppressing Ps formation. Alternatively, given the higher Er concentration (the maximum Er concentration for the sample is ~1%) in the SiO_2 layer, Er ions might occupy spaces, in which Ps would be formed, annihilating Ps formation sites. Ion-implantation-induced defects in SiO_2 are produced by very complicated interaction between collisional and electronic processes,[23] and require further study.

B. Defects in the Si substrate

We note that the ESR signal attributed to amorphous Si is observed for the as-implanted sample [Fig. 5, spectrum (b)]. The depth profile of implanted Er ions calculated by TRIM peaks at 21 nm from the surface and is distributed with a FWHM of ~10 nm. It also shows that no Er ions are present in the Si substrate. However, ESR data in Fig. 5 suggest that defects induced by Er ion implantation extend to

[This article is copyrighted as indicated in the article. Reuse of AIP content is subject to the terms at: http://scitation.aip.org/termsconditions. Downloaded to] IP: 157.111.48.196 On: Sat, 30 Jan 2016 06:38:52

the Si substrate. Positron trapping at an open-volume-type defect in Si with no Ps formation generally enhances the S parameter due to the increased probability of positron annihilation with low-momentum valence electron. S parameters of the as-implanted sample at positron energies of 4.4–10 keV (Fig. 3), however, are decreased in comparison with the unimplanted sample.

Damage distributions in ion-implanted materials were compared with average ion-implantation depth R_p calculated using TRIM to study effects of implanted ion species and energies on damage profile.[26] It was revealed that the ratio of thickness for damaged layer X_d to R_p proportionally increases with decreasing $\log \epsilon$ if $\epsilon < 10$; here, ϵ is Lindhard's dimensionless reduced energy given by

$$\epsilon = \frac{a_0 E}{Z_1 Z_2 e^2} \frac{M_2}{M_1 + M_2}, \tag{1}$$

where E is the energy of the incident particle, a_0 is the screening length, M_1 and $Z_1 e$ are the mass and charge of the incident particle, and M_2 and $Z_2 e$ are those of the target atom.[27] In a material that consists of n elements, we assumed that reduced energy is expressed by

$$\epsilon = \sum_{i=1}^{n} a_i \epsilon_i, \tag{2}$$

where a_i is the atomic fraction and ϵ_i the reduced energy for element i. The ratio of X_d to R_p was ~1 for $\epsilon = 10$, whereas it was ~2 for $\epsilon = 1$. As ϵ for 30 keV Er^+-implanted SiO_2 is calculated to be 0.03 from Eqs. (1) and (2), the ratio is estimated to be ~3.5, if we linearly extrapolate previous plots. Taking $R_p = 21$ nm into consideration, the thickness of the damaged layer is calculated to be ~70 nm, which is thicker than the thickness of the SiO_2 layer. Thus, although the S parameter is reduced, it is likely that defects are produced in the Si substrate by 30 keV Er ion implantation.

We could attribute the reduction of S to the complex formation of the defect with oxygen. It is well known that the presence of oxygen at the positron annihilation site reduces the S parameter due to the increased probability of positron annihilation with high momentum core electrons of oxygen.[28,29] The information on atoms with positron annihilation is obtained from Doppler broadening annihilation spectra in the high-momentum region.[29] Figure 6 shows the Doppler-broadening ratio curves of the spectra averaged over positron energies of 4.5–6.7 keV for the implanted sample relative to the spectrum for bulk Si. Since the characteristic peak due to positron annihilation with oxygen is at 514 keV,[29] the presence of oxygen at the positron annihilation site in the as-implanted sample is confirmed. Implanted 30 keV Er ions lose most of their energy (~90%) by the collisional process (rather than the electronic process), followed by the formation of recoil atoms. We infer that energetic oxygen atoms produced in the SiO_2 layer as recoil atoms are implanted into the Si substrate and responsible for the formation of vacancy-oxygen complex. The annealing behavior of the peak at 514 keV in Fig. 6 suggests that certain oxygen related defects are annealed out at 300 °C possibly by dissolution of oxygen into Si. The enhancement of the peak at 600 °C may be due to the formation of other types of oxygen-related defects such as multivacancy-multioxygen complexes at this temperature.

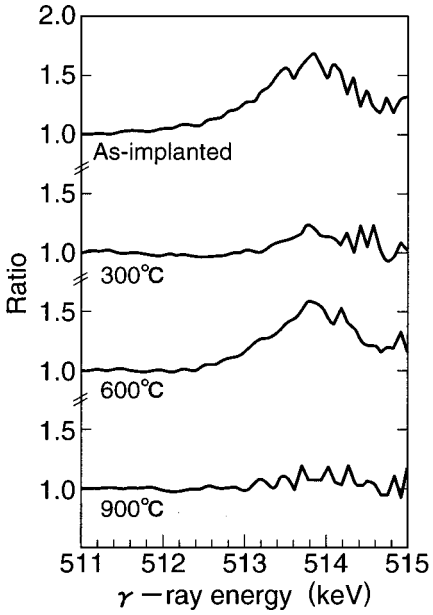

FIG. 6. Annealing temperature dependence of Doppler-broadening ratio curves for the 1.5×10^{15} Er/cm^2 sample to the spectrum for bulk Si.

C. Effect of defects on Er^{3+} luminescence

In the presence of defects, luminescence at a wavelength of 1.54 μm from the Er ion is weakened because of nonradiative transitions from the excited level of Er^{3+} ion to acceptor states produced by defects.[6] If the nonradiative transition does not depend on the distance between the Er^{3+} ion and acceptor, luminescence intensity I is given by $I = A\tau/\tau_{\mathrm{rad}}$, with A a constant depending on quantum efficiency and Er ion concentration, etc., τ the measured luminescence lifetime, and τ_{rad} the lifetime of the radiative transition in the absence of nonradiative processes.[6] Since measured lifetime τ is expressed as $(1/\tau_{\mathrm{rad}} + k[D])^{-1}$ with k a constant and $[D]$ a defect concentration, the above relationship for luminescence intensity I indicates that the luminescence intensity decreases monotonically with increasing defect concentration.

We measured cathodoluminescence (CL) for SiO_2:Er/Si samples at a wavelength of 1.54 μm due to the intra-$4f$ transition between $^4I_{13/2}$ and $^4I_{15/2}$. All measurements were carried out at room temperature with a system detailed elsewhere.[17] Figure 7 shows the annealing temperature dependence of CL luminescence intensity for samples with doses of 3.0×10^{14} and 1.5×10^{15} Er/cm^2. Taking the discussion on defects in Sec. III A into consideration, it turns out that the annealing temperature dependence of CL intensity in Fig. 7 does not coincide with that of defects. The most pronounced enhancement in CL intensity is observed, for example, between 600 and 900 °C, whereas no significant change in the S parameter is observed at this temperature range and ESR-detectable defects are annealed out up to 600 °C. It should be also noted that as-implanted samples at

[This article is copyrighted as indicated in the article. Reuse of AIP content is subject to the terms at: http://scitation.aip.org/termsconditions. Downloaded to] IP: 157.111.48.196 On: Sat, 30 Jan 2016 06:38:52

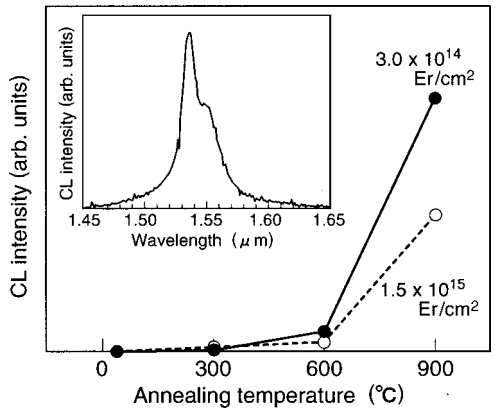

FIG. 7. Cathodoluminescence (CL) peak intensity at 1.54 μm measured at room temperature for the SiO_2/Si implanted with doses of 3.0×10^{14} and 1.5×10^{15} Er/cm^2 as a function of annealing temperature. The accelerating voltage and electron beam current were 10 kV and 10–15 nA. Inset: typical CL spectrum (dose: $\Phi=1.5\times10^{15}$ Er/cm^2, annealing temperature: 900 °C). The spectrum is composed of two peaks at $\lambda=1.54$ μm and $\lambda=1.55$ μm, typically seen as $^4I_{13/2}\rightarrow{}^4I_{15/2}$ internal transitions of Er^{3+} during luminescence measurements. No significant difference in spectral shape by annealing temperature was observed.

30 keV are not luminescent (Fig. 7). This is opposite to our previous result, that intense luminescence is observed for as-implanted SiO_2(500 nm)/Si implanted with 300 keV Er ions at a dose of 1.5×10^{15} Er/cm^2.[30] The S parameter in the SiO_2 layer for the 300 keV Er sample is nearly equal to that for the as-implanted 30 keV Er sample with the same dose. The presence of defects detected by ESR and positron measurements does not, therefore, significantly affect CL intensity.

The simple relationship between luminescence intensity and defect concentration $I=A/(1+\tau_{rad}k[D])$ is valid only when all Er ions are in the same state. Er ions are surrounded by defects if self-annealing caused by the implanted ion itself is not sufficient to recover defects. Remaining defects in the nearest neighbor shell of Er ions should shorten the lifetime of the excited Er ion because of the fast transition from the excited state of Er ion to acceptor levels of defects. Thus, emission from these Er ions is expected to be very weak and their contribution to the luminescence at 1.54 μm may be negligible. In fact, the Er ion is required to be in a suitably defect-free state coordinated with six oxygen atoms to show the luminescence.[7,31] Taking account of such Er ions, the expression for the overall luminescence intensity could be replaced by $I=Af(\mathrm{Er})/(1+\tau_{rad}k[D])$, where $f(\mathrm{Er})$ is the fraction of Er ions suitably coordinated with surrounding atoms.

To obtain an optically active defect-free configuration, atomic mobility should be indispensable. Snoeks *et al.* showed that effective viscosity η of SiO_2 during ion irradiation decreases with increasing nuclear energy loss, i.e., $\eta\propto S_{n,max}^{-1.1}$, where $S_{n,max}$ is the maximum nuclear energy loss.[32] The defect-free configuration of Er ions may be attained during ion implantation only when the effective viscosity is sufficiently reduced to make atoms mobile. TRIM calculations show that $S_{n,max}$ for 30 keV Er into SiO_2(0.54 keV/nm/ion) is roughly half that for 300 keV Er (1.24 keV/nm/ion). This suggests that Er ions implanted with an energy of 30 keV cannot make the surrounding atoms mobile because of lower $S_{n,max}$ and do not attain optically activated configuration during ion implantation. We consider defects surrounding the Er ions which start to be annealed out below 600 °C. The defect concentration decreases during annealing between 600 and 900 °C, which enhances luminescence intensity $I=Af(\mathrm{Er})/(1+\tau_{rad}k[D])$ by increasing of $f(\mathrm{Er})$.

IV. CONCLUSION

Defects in SiO_2 (48 nm)/Si implanted by 30 keV Er ions at doses of 3.0×10^{14} and 1.5×10^{15} Er/cm^2 were studied using variable-energy positron annihilation Doppler broadening and ESR, and the results were compared with cathodoluminescence data. Annealing treatment was required for the samples to show measurable luminescence at a wavelength of 1.54 μm. The most pronounced enhancement in CL intensity observed between 600 and 900 °C was not accompanied by the recovery of defects detected by positron and ESR. As-implanted SiO_2/Si with higher implantation energy (300 keV Er) was highly luminescent in spite of a lower S parameter for the SiO_2 layer. These results indicate that the presence of positron and ESR-detectable defects does not significantly influence Er ion luminescence intensity. TRIM calculations revealed that the maximum nuclear energy loss for 30 keV Er into SiO_2 was roughly half that for 300 keV Er, suggesting that effective viscosity, related to atomic mobility, for the former condition was not high enough to anneal out defects surrounding Er ions during implantation. Proper control of defects surrounding Er ions in the SiO_2 layer should be thus important in optimizing the luminescence of Er ions in a thin SiO_2 layer ($<$50 nm).

[1] P. J. Mears, L. Reekie, I. M. Jauncey, and D. N. Payne, Electron. Lett. **23**, 1026 (1987).
[2] H. Ennen, J. Schneider, G. Pomrenke, and A. Axmann, Appl. Phys. Lett. **43**, 943 (1983).
[3] H. Ennen, G. Pomrenke, A. Axmann, K. Eisele, W. Haydl, and J. Schneider, Appl. Phys. Lett. **46**, 381 (1983).
[4] S. Wang, A. Eckau, E. Neufeld, R. Carius, and Ch. Buchal, Appl. Phys. Lett. **71**, 2824 (1997).
[5] A. Polman, D. C. Jacobson, D. J. Eaglesham, R. C. Kistler, and J. M. Poate, J. Appl. Phys. **70**, 3778 (1991).
[6] A. Polman and J. M. Poate, J. Appl. Phys. **73**, 1669 (1993).
[7] A. Polmam, J. Appl. Phys. **82**, 1 (1997).
[8] *Positron in Solids*, edited by P. Hautojarvi (Springer, Berlin, 1979).
[9] *Positron Solid-State Physics*, edited by W. Brandt and A. Dupasquier (North-Holland, Amsterdam, 1983).
[10] M. J. Puska and R. M. Nieminen, Rev. Mod. Phys. **66**, 841 (1994).
[11] *Positron Spectroscopy of Solids*, edited by A. Dupasquier and A. P. Mills, Jr. (IOS, Amsterdam, 1995).
[12] P. J. Schultz and K. G. Lynn, Rev. Mod. Phys. **60**, 701 (1988).
[13] P. Asoka-Kumar, K. G. Lynn, and D. O. Welch, J. Appl. Phys. **76**, 4935 (1994).
[14] Y. Saitoh, S. Tajima, I. Takada, K. Mizuhashi, S. Uno, K. Ohkoshi, Y. Ishii, T. Kamiya, K. Yotumoto, R. Tanaka, and E. Iwamoto, Nucl. Instrum. Methods Phys. Res. B **89**, 23 (1994).
[15] J. P. Biersack and L. G. Haggmark, Nucl. Instrum. Methods **174**, 257 (1980).
[16] Y. Kobayashi, I. Kojima, S. Hishita, T. Suzuki, E. Asari, and M. Kitajima, Phys. Rev. B **52**, 823 (1995).
[17] T. Sekiguchi and K. Sumino, Rev. Sci. Instrum. **66**, 4277 (1995).
[18] A. Uedono, L. Wei, S. Tanigawa, R. Suzuki, H. Ohgaki, T. Mikado, T. Kawano, and Y. Ohji, J. Appl. Phys. **75**, 3822 (1994).

[This article is copyrighted as indicated in the article. Reuse of AIP content is subject to the terms at: http://scitation.aip.org/termsconditions. Downloaded to] IP: 157.111.48.196 On: Sat, 30 Jan 2016 06:38:52

[19] *Positron and Positronium Chemistry*, edited by D. M. Schrader and Y. C. Jean (Elsevier, Amsterdam, 1988).
[20] R. Suzuki, Y. Kobayashi, K. Awazu, T. Mikado, M. Chiwaki, H. Ohgaki, and T. Yamazaki, Nucl. Instrum. Methods Phys. Res. B **91**, 410 (1994).
[21] O. E. Mogensen, J. Chem. Phys. **60**, 998 (1974).
[22] M. Hasegawa, M. Tabata, M. Fujinami, Y. Ito, H. Sunaga, S. Okada, and S. Yamaguchi, Nucl. Instrum. Methods Phys. Res. B **116**, 347 (1996).
[23] E. P. EerNisse and C. B. Norris, J. Appl. Phys. **45**, 5196 (1974).
[24] J. Ch. Abbe, G. Duplatre, A. G. Maddock, J. Talamoni, and A. Haessler, J. Inorg. Nucl. Chem. **43**, 2603 (1981).
[25] A. G. Maddock, J. Ch. Abbe, G. Duplatre, and A. Haessler, Chem. Phys. **26**, 163 (1977).
[26] K. Hirata, Y. Kobayashi, S. Hishita, and Y. Saitoh, Nucl. Instrum. Methods Phys. Res. B **164–165,** 471 (2000).
[27] J. Lindhard, V. Nielsen, and M. Scharff, K. Dan. Vidensk. Selsk. Mat. Fys. Medd. **36**, 10 (1968).
[28] M. Fujinami, Phys. Rev. B **53**, 13047 (1996).
[29] U. Myler, R. D. Goldberg, A. P. Knights, D. W. Lawther, and P. J. Simpson, Appl. Phys. Lett. **69**, 3333 (1996).
[30] A. Kawasuso, H. Arai, K. Hirata, T. Sekiguchi, Y. Kobayashi, and S. Okada, Radiat. Phys. Chem. **58**, 615 (2000).
[31] M. A. Marcus and A. Polman, J. Non-Cryst. Solids **136**, 260 (1991).
[32] E. Snoeks, T. Weber, A. Cacciato, and A. Polman, J. Appl. Phys. **78**, 4723 (1995).

[This article is copyrighted as indicated in the article. Reuse of AIP content is subject to the terms at: http://scitation.aip.org/termsconditions. Downloaded to] IP: 157.111.48.196 On: Sat, 30 Jan 2016 06:38:52